

Ab initio Molecular Dynamics Along the Intrinsic Reaction Path: A New Perspective on Old Reactions

Ab Initio Molecular Dynamics

● **Car-Parrinello *ab initio* MD:** Frictionless dynamics for the wave functions handles electronic and atomic structure on equal footing within classical Lagrangian mechanics. The electronic structure is treated at the DFT⁷ level.

$$M_j \ddot{R}_j = -\frac{\partial E[R_j, \{\psi_j\}]}{\partial R_j}, \quad m_j \ddot{\psi}_j = -\frac{\delta E[R_j, \{\psi_j\}]}{\delta \psi_j} - \sum_i |\psi_i\rangle \lambda_{ij}$$

● **Projector-Augmented Wave (PAW) method:**⁸ Basis set composed of plane waves, augmented with atom-centred functions to describe accurately the nodal structure of the wave function near the nuclei. The frozen-core approximation is used.

$$|\psi_n\rangle = |\tilde{\psi}_n\rangle + \sum_k |\phi_k\rangle \langle \tilde{p}_k | \tilde{\psi}_n\rangle - \sum_k |\tilde{\phi}_k\rangle \langle \tilde{p}_k | \tilde{\psi}_n\rangle$$

Reaction Paths

- **Zero-temperature path:** The intrinsic reaction path (IRP)⁴ is obtained by following the steepest-descent path from the transition state.
- **Slow-growth thermodynamic integration:**⁵ Dynamics at finite temperature along an arbitrary, presupposed reaction coordinate λ . The change in free energy is obtained by integrating the force of constraint needed to keep the system at a given value of λ .

$$\Delta A = \int d\lambda \frac{\partial A(\lambda)}{\partial \lambda} \xrightarrow{\text{slow growth}} \sum_i^M f_i^c \Delta \lambda_i, \quad \Delta \lambda_i = \frac{\lambda_i - \lambda_0}{M}$$

● Problem: Hysteresis between forward- and backward run due to insufficient sampling and/or bad choice of reaction coordinate.

● Optimal reaction coordinate: Intrinsic reaction coordinate (IRC).

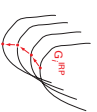
- **Slow growth along the intrinsic reaction path:**⁶ Given a series of points in configuration space along the IRP, $\{X_i^{\text{IRP}}\}$, the displacements in each simulation step are constrained to be orthogonal to the IRP direction, \mathbf{G}^{IRP} .

$$(R_i - X_i^{\text{IRP}}) \cdot \mathbf{G}_i^{\text{IRP}} = 0; \quad \mathbf{G}_i^{\text{IRP}} \propto (X_{i+1}^{\text{IRP}} - X_{i-1}^{\text{IRP}})$$

The constraint condition can be expressed as a linear constraint.

$$R_i \cdot \mathbf{G}_i^{\text{IRP}} = X_i^{\text{IRP}} \cdot \mathbf{G}_i^{\text{IRP}} = c$$

- In the slow-growth simulation, the constraint vector, \mathbf{G}^{IRP} , and the value of the constraint, c , are changed in each time step.



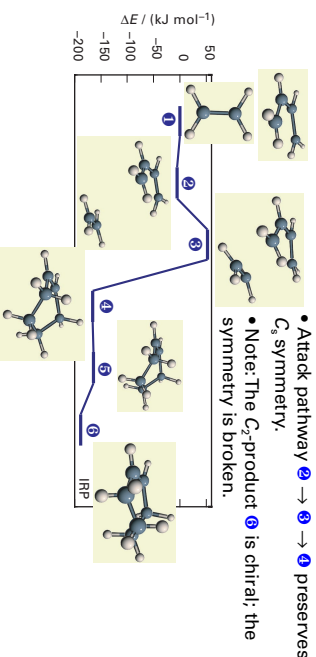
References

- R. Car, M. Parrinello, *Phys. Rev. Lett.* 1985, 55, 2471–2474.
- (a) LDA correlation: J. P. Perdew, Y. Wang, *Phys. Rev. B* 1992, 46, 12944–12946; (b) GGA exchange: A. D. Becke, *Phys. Rev. A* 1988, 38, 3098–3100; (c) GGA correlation: J. P. Perdew, *Phys. Rev. B* 1986, 33, 882–884; J. P. Perdew, *Phys. Rev. B* 1986, 34, 7100.
- P. E. Blöchl, *Phys. Rev. B* 1994, 50, 17533–17539.
- (a) K. Fukui, *J. Phys. Chem.* 1970, 74, 4161–4163; (b) K. Fukui, *Acc. Chem. Res.* 1981, 14, 363–368.
- (a) T. Straatsma, H. J. C. Berendsen, J. M. Postma, *J. Chem. Phys.* 1986, 85, 6720–6727; (b) M. Sprik, G. Cicciotti, *J. Chem. Phys.* 1988, 109, 737–744.
- A. Michalak, T. Ziegler, *J. Phys. Chem. A* 2001, 105, 4339–4343.

Diels-Alder Reaction

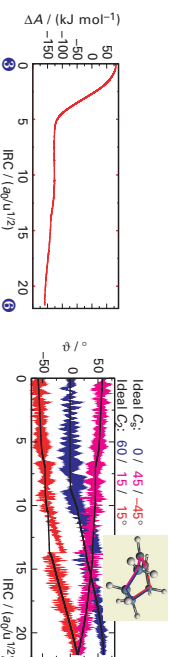
● Intrinsic reaction path

- Separated reactants: Ethene + *s-cis*-butadiene at infinite separation
- Pre-reaction complex: Endpoint of IRP
- Diels-Alder transition state
- C*₂-cyclohexene: IRP is trapped in this shallow minimum!
- Transition state *C*₂ → *C*₂
- C*₂-cyclohexene: The final product



● Finite-temperature simulations along the IRP

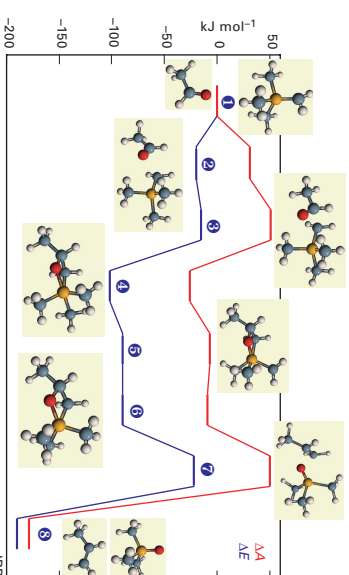
- **Diels-Alder attack 2 → 3 → 4:**
 - Dynamics follows the IRP
 - Structural changes along the IRP illustrate changes in hybridization and bonding character.
 - *A* from thermodynamic integration agrees well with results from static calculations.
- However: There is no *C*₂-minimum (4) and no second TS (5) on the free-energy surface! *C*₂-cyclohexene (4) is formed directly.
 - Free-dynamics runs from TS 3 yield either of the enantiomers of 4 with equal probability.
 - The decision for either enantiomer is taken only after TS 3; the bond forming process retains *C*₂ symmetry.
- **Simulation along 4 (→ 5 → 6) → 6:**
 - Conversion *C*₂ → *C*₂ monitored by changes in torsion angles.



Wittig Reaction

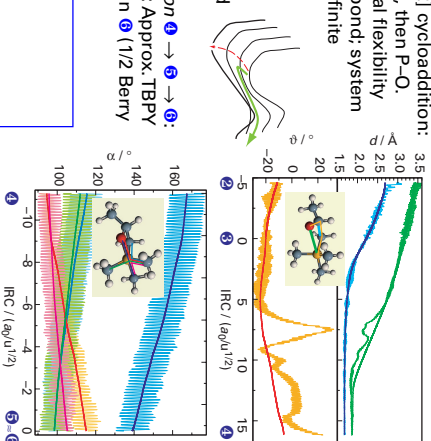
● Intrinsic reaction path

- Separated reactants: Acetaldehyde + methylenetriethylphosphorane
- Pre-reaction complex
- Transition state for [2+2] cycloaddition
- Oxaphosphetane I
- Transition state for Berry pseudorotation at P
- Oxaphosphetane II
- Transition state for [2+2] cycloreversion
- Products: Propene + trimethylphosphane oxide



● Finite-temperature simulations along the IRP

- **Oxaphosphetane formation 2 → 3 → 4:**
 - Asynchronous [2+2] cycloaddition: C–C bond forms first, then P–O.
 - High conformational flexibility about incipient C–C bond; system deviates from IRP at finite temperature!
 - Strategies to keep system close to IRP: Lower *T*, additional constraints, modified potential.
- **Berry pseudorotation 4 → 5 → 6:**
 - Configuration at P: Approx. TBPY in 4 → approx. SPY in 5 (1/2 Berry cycle).



Summary

- IRP provides ideal reaction coordinate for slow-growth simulations.
- Allows determination of free energies and gives detailed insight into dynamical aspects of the reaction.
- Deviations between finite-temperature path and IRP identify characteristic features of the free-energy surface, such as easily accessible alternative reaction channels.